JACC Vol. 17, No. 6
May 1991:1416–23

Scintigraphic Assessment of Sympathetic Innervation After Transmural Versus Nontransmural Myocardial Infarction

MICHAEL W. DAE, MD, JOHN M. HERRE, MD, FACC, J. WILLIAM O'CONNELL, MS, ELIAS H. BOTVINICK, MD, FACC, DAVID NEWMAN, MD, LOUISA MUNOZ, MD

San Francisco, California

To evaluate the feasibility of detecting denervated myocardium in the infarcted canine heart, the distribution of sympathetic nerve endings using I-123 metaiodobenzylguanidine (MIBG) was compared with the distribution of perfusion using thallium-201, with the aid of color-coded computer functional map in 16 dogs. Twelve dogs underwent myocardial infarction by injection of vinyl latex into the left anterior descending coronary artery (transmural myocardial infarction, n = 6), or ligation of the left anterior descending coronary artery (nontransmural myocardial infarction, n = 6). Four dogs served as sham-operated controls. Image patterns were compared with tissue norepinephrine content and with histofluorescence microscopic findings in biopsy specimens.

Hearts with transmural infarction showed zones of absent MIBG and thallium, indicating scar. Adjacent and distal regions showed reduced MIBG but normal thallium uptake, indicating viable but denervated myocardium. Denervation distal to infarction was confirmed by reduced norepinephrine content and absence of nerve fluorescence. Nontransmural myocardial infarction showed zones of wall thinning with decreased thallium uptake and a greater reduction or absence of MIBG localized to the region of the infarct, with minimal extension of denervation beyond the infarct. Norepinephrine content was significantly reduced in the infarct zone, and nerve fluorescence was absent.

These findings suggest that 1) MIBG imaging can detect viable and perfused but denervated myocardium after infarction; and 2) as opposed to the distal denervation produced by transmural infarction, nontransmural infarction may lead to regional ischemic damage of sympathetic nerves, but may spare subepicardial nerve trunks that course through the region of infarction to provide a source of innervation to distal areas of myocardium.

(J Am Coll Cardiol 1991;17:1416–23)

The sympathetic nervous system is believed to play an important role in normal cardiac function and cardiac pathophysiology (1). It was recently demonstrated (2) that transmural myocardial infarction produces necrosis of nerves coursing in the epicardium leading to viable but denervated myocardium. This partial denervation may produce imbalanced sympathetic innervation, which during enhanced sympathetic tone may predispose the heart to arrhythmia (3).

The distribution of myocardial innervation after infarction has not been investigated carefully, particularly in the intact heart. Several recent studies (4–7) show the feasibility of imaging the distribution of myocardial sympathetic nerves with use of radiolabeled metaiodobenzylguanidine (MIBG). The purpose of this investigation was: 1) to evaluate the feasibility of detecting denervated myocardium in the infarcted canine heart with MIBG, and 2) to test the hypothesis that transmural but not nontransmural infarction leads to denervated but viable myocardium. To facilitate the analysis of innervation, the distribution of myocardial perfusion was assessed simultaneously with use of thallium-201.

Methods

We compared the myocardial distribution of sympathetic nerves imaged with I-123 MIBG with the distribution of myocardial perfusion imaged with thallium-201, with the aid of color-coded computer functional maps.

Study dogs. Studies were performed on 16 conditioned adult dogs that weighed 10 to 26 kg. Twelve dogs underwent myocardial infarction by either 1) injection of vinyl latex into the left anterior descending coronary artery (n = 6), or 2) ligation of this artery (n = 6). In a previous investigation, we (3) found that a dense, homogeneous transmural infarction resulted after the injection of vinyl latex into this artery. When infarction was produced by ligation of the vessel without latex injection, a nontransmural infarction routinely resulted. These models were chosen in order to assess the

From the Departments of Medicine, Cardiovascular Division, and Radiology, Section of Nuclear Medicine, and the Cardiovascular Research Institute of the University of California, San Francisco, San Francisco, California. Dr. Dae is supported in part by a FIRST Award from the National Institutes of Health, Bethesda, Maryland and a Pre-Tenure Award from the Academic Senate, University of California, San Francisco. This work was supported in part by a grant from the Fannie Ripple Foundation, Madison, New Jersey; Grants HL-38105 and HL-25847 from the National Institutes of Health; the Academic Senate Committee on Research, University of California, San Francisco; and Clinical Grant CG-89007 from Du Pont, Bellerica, Massachusetts. Dr. Newman is supported by a fellowship grant from the Medical Research Council, Toronto, Ontario, Canada. Dr. Munoz is supported by a FISS fellowship grant from the Health Ministry, Madrid, Spain.

Manuscript received April 17, 1990; revised manuscript received November 2, 1990, accepted December 5, 1990.

Address for reprints: Michael W. Dae, MD, Box 0252, University of California, San Francisco, San Francisco, California 94143.

0735-1097/91/$3.50

effects of transmural versus nontransmural infarction on sympathetic innervation. Four dogs served as sham-operated control animals.

Surgical procedures. The dogs were anesthetized with sodium pentobarbital (30 mg/kg body weight), intubated and ventilated mechanically (Harvard respirator) with a mixture of room air and oxygen. The surface electrocardiographic (ECG) lead II was monitored throughout the procedure. Under sterile conditions, a thoracotomy was performed in the left fourth intercostal space. The pericardium was opened, and a cradle was made with 2-0 silk sutures by attaching the margins of the pericardium to the margins of the thoracotomy. The left anterior descending coronary artery was identified and isolated by blunt dissection just distal to the takeoff of the first diagonal branch. Myocardial infarction was then produced by one of two methods:

Latex infarction model (8). After isolation, the left anterior descending coronary artery was partially occluded for 20 min. It was then occluded totally, and vinyl latex (1 to 3 cc) (Carolina Biological Supply) was injected distal to the ligature. The dog was observed with the chest open for spontaneous arrhythmia for 30 min, after which the pericardium and the chest were closed, air was evacuated and the dog was allowed to recover. Ventricular arrhythmias were managed with lidocaine.

Ligation model (9). After isolation, the left anterior descending coronary artery was occluded partially for 20 min and then completely. The dog was observed, arrhythmias were treated and the pericardium and chest were closed as described earlier.

For the sham-operated control dogs, the left anterior descending coronary artery was isolated using blunt dissection as described. A ligature was passed under the coronary artery and removed. The dogs were observed and treated as before.

Imaging protocol. Fourteen of 16 dogs were studied a mean of 6 days (range 4 to 12) after surgery. Two dogs (ligation group) were studied 3 and 5 weeks after surgery, respectively. The dogs were anesthetized with pentobarbital, intubated and ventilated with a Harvard respirator. Four to 6 mCi of I-123 MIBG was injected intravenously, followed by the acquisition of 5 min planar images in the anterior, 40° and 70° left anterior oblique projections, using a Siemens LEM portable gamma camera, fitted with a 20° slant-hole collimator and interfaced to an IBM PC-XT–based portable computer acquisition system (Harpootlian Associate). The energy window was set at the 159 keV photopeak of I-123. Three hours after injection of MIBG, the planar images were repeated, followed by the injection of 1.5 to 2 mCi of thallium-201. The 3 h delay allows nonneuronally bound MIBG to wash out from the heart, leaving neuronally bound MIBG, which has a much slower washout rate (10). Five minute planar images of I-123 MIBG (159 keV), followed by 5 min planar images of thallium-201 (80 keV), were acquired in registration in each projection. Prior phantom studies using equicurie amounts of I-123 and thallium-201 showed 5.7% spillover of I-123 counts into the thallium-201 window and 12.3% spillover of thallium counts into the I-123 window. The net result of the spillover may be an underestimation of the degree of denervation due to the presence of thallium counts in the I-123 window. This is partly compensated for by administering a larger dose of I-123 MIBG than of thallium (4 to 6 mCi of I-123 MIBG vs. 1.5 to 2 mCi of thallium). We previously demonstrated the feasibility of detecting denervated myocardium scintigraphically (6).

Myocardial biopsy. After imaging, the dogs were killed with an injection of saturated potassium chloride, and the hearts were excised rapidly and sliced transversely into approximately 1 cm sections. The region of infarction was visible on the gross specimens. The left ventricular free wall, apical and lateral to the infarct (border zone), and the posterior basal region (control region) were biopsied and analyzed for norepinephrine content in four of the hearts with latex-induced infarction and four of the hearts with coronary ligation-induced infarction. Biopsy samples were obtained from similar regions in the sham-operated control dogs. In the hearts with ligation-induced infarction, an additional sample was taken from within the infarct territory for norepinephrine content analysis.

Additional samples were removed from one of the hearts with latex-induced infarction and four of the hearts with ligation-induced infarction and processed for histofluorescence microscopy as described later. After biopsy, the myocardial slices were imaged directly for MIBG and thallium activity (5 min acquisition for each isotope).

Histologic classification of infarction. The myocardial slices were fixed in 10% buffered formalin. After fixation, transmural biopsy specimens were taken from the anterior, lateral and posterobasal walls of the left ventricle, dehydrated, and embedded in paraffin for light microscopy. Five micron sections were stained with hematoxylin-eosin and examined histologically. Myocardial infarcts were classified as *transmural* if they showed uniform myocardial necrosis extending in continuity from the endocardium to the epicardium and *nontransmural* if they showed nonhomogeneous myocardial necrosis characterized by a prominent epicardial rim of viable (histologically normal) myocardium and a complex histologic pattern of viable myocardium interdigitating with necrotic myocardium.

Norepinephrine content analysis. Biopsy samples were weighed, and stored in 2 ml of 0.1*N* perchloric acid at −70° C, until analyzed. Just before analysis, the tissue was homogenized in a polytron and the supernatant was analyzed by high performance liquid chromatography (SmithKline Bio-Science Laboratories).

Histofluorescence microscopy. Tissue samples were immersed in O.C.T. compound embedding medium (Miles Laboratories), frozen in isopentane chilled to −125° in liquid nitrogen, and stored at −70°C until the time of study. The frozen pieces of tissue were sectioned on a cryostat to 10 μm and placed on room temperature glass slides. The slides

were immersed in a 1% glyoxylic acid solution according to the method of DeLaTorre (11), then dried, mounted with mineral oil and a cover slip, and viewed with a fluorescence microscope equipped with a catecholamine fluorescence filter. Adjacent frozen sections were mounted on glass slides, dried on a hot plate and stained with hematoxylin-eosin for histologic assessment.

Computer functional maps. Color-coded computer functional maps were generated with use of a PDP 11/40 computer (Digital Equipment Corp.) to display the simultaneous distribution of adrenergic nerve uptake from the 3 h delayed MIBG images and myocardial perfusion from the thallium images. The method for forming the functional maps is described in detail elsewhere (6). The early MIBG images were not used for this analysis.

First, the brightest pixel in the MIBG image was normalized to the brightest pixel in the thallium image. The functional maps were then processed in two steps: 1) correction of background in each image, and 2) calculation of a color functional map, in which each pixel encodes two variables: *a) Polar magnitude* [$M = \sqrt{(I_1^2 + I_2^2)}$] measures composite signal strength and determines pixel intensity, or brightness, where I_1 and I_2 represent the counts from the MIBG and thallium-201 images, respectively. Thirty-one intensity levels are used in the color maps. In this manner, pixels with very low counts, as in infarcted regions, will appear as very low intensity in the maps, whereas better perfused regions will appear with greater intensity. *b) Polar angle* [$A = \arctan (I_2/I_1)$] measures the relative signal strengths of the combination of I_1 and I_2, and determines the hue of each pixel. Seven hues encoding seven polar angle intervals are used in the maps. Pixels with 100% MIBG are color coded blue, 50% MIBG red and very low levels of MIBG green. In this manner, equivalent amounts of MIBG and thallium were coded red, representing balanced innervation, whereas decreasing amounts of MIBG relative to thallium were coded yellow to green, indicating increasing denervation. A relative excess of MIBG would be coded purple to blue.

Additionally, with this color scheme, the degree of denervation can be quantitated on a relative basis from the functional maps by examining the amount of reduction in MIBG compared with that in the normal region (red). If the red region represents 100% MIBG, the mid range of the yellow hue represents 76% of normal MIBG, light green 50% of normal MIBG and dark green 18% of normal MIBG.

As mentioned, relative degrees of perfusion are encoded by intensity. As a consequence, the brightest area in the maps represents areas of greatest flow, and decreased intensity represents areas of *relatively* reduced flow. Hence, infarcted regions will appear as defects in the functional maps. In summary, a relative decrease in MIBG versus thallium is color coded in the functional maps, and a relative decrease in perfusion is intensity coded. However, these maps do not reflect whether absolute thallium uptake (flow) is normal.

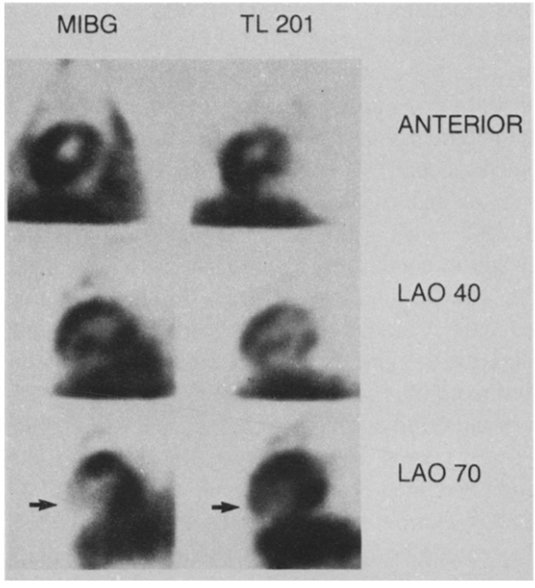

Figure 1. Planar images of MIBG (**left**), and thallium uptake (**right**) in three projections from a dog studied 5 days after latex injection into the left anterior descending coronary artery. For each projection the two images were recorded in registry. A large region of decreased MIBG uptake is present, whereas the corresponding thallium image appears more homogeneous. This is best demonstrated in the left anterior oblique (LAO) 70° projection (**arrows**).

Statistical analysis. Norepinephrine contents from basal control, peri-infarcted, and infarcted regions were expressed as mean values ± SD. Basal and infarcted and basal and peri-infarcted regions were compared using a one-way analysis of variance. For the hearts in which basal and peri-infarct regions were analyzed and in the sham-operated control dogs, an unpaired *t* test was used for comparison. Norepinephrine contents were related to the MIBG/thallium distributions on the functional maps.

Results

Latex model. All of the hearts injected with latex showed gross visible evidence of homogeneous transmural infarction of varying degree. This was confirmed histologically as necrotic and scarred myocardium in a transmural distribution. As seen in Figure 1, all of the latex-injected hearts showed regions of a greater reduction in MIBG than in thallium activity. This pattern was evident on the functional maps as regions of yellow to green (Fig. 2), providing scintigraphic evidence of denervated but viable myocardium. The functional maps showed transmural regions with no thallium or MIBG (Fig. 2B) consistent with scar or necrosis. The pattern of denervation was fairly uniform in these transmural infarcts, with a broad area of denervation located apical and lateral to the scar (Fig. 2B). Regions proximal to the infarct area showed normal innervation. The areas showing scintigraphic denervation (reduced MIBG with relatively greater perfusion) had significantly reduced norepinephrine content, compared with posterobasal control

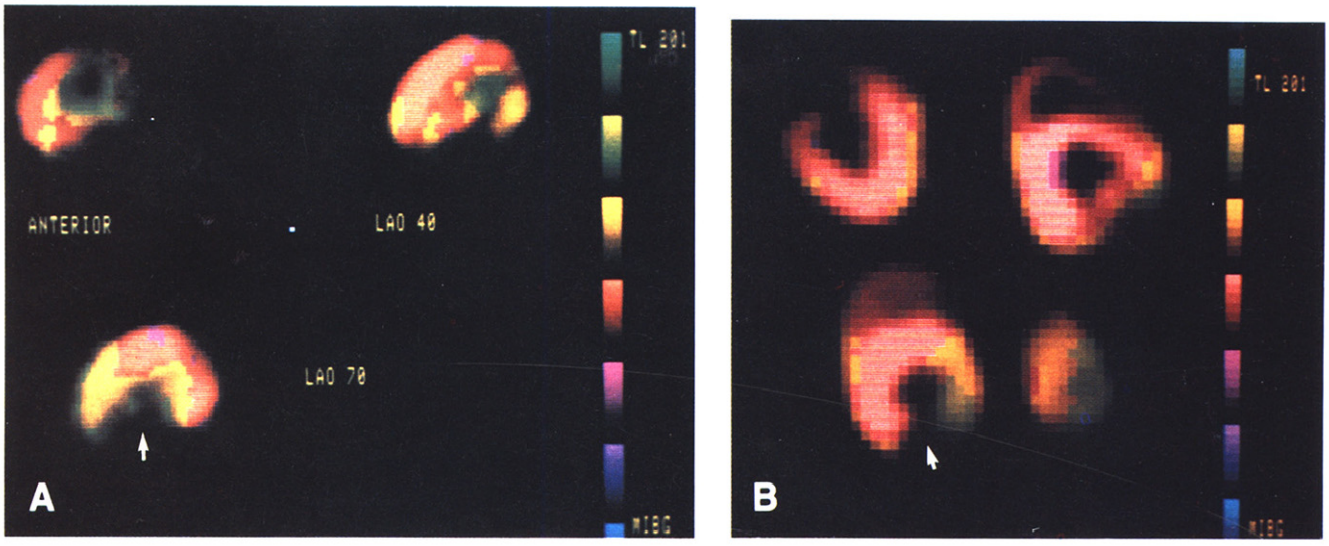

Figure 2. A, Color functional maps from the planar projections shown in Figure 1. Regions of balanced perfusion and MIBG uptake (normal innervation) are shown in red. Regions showing a greater reduction in MIBG relative to thallium are shown in yellow to green. This is again best demonstrated in the left anterior oblique (LAO) 70° projection. The area devoid of activity in the free wall of the left ventricle represents scar (**arrow**). **B,** Functional maps of the myocardial slices. Note the area of absent activity in the slice proximal to the apex (**arrow**). This represents a region of transmural scar. Adjacent and distal to this region of scar is an area of denervated myocardium, represented by the yellow to green color. Note also that the intensity of this denervated area is bright and the thickness of the wall is similar to that in normal, uninvolved regions.

regions (112 ± 139 vs. 698 ± 66 ng/g, $p < 0.002$). Histologically, these denervated regions were normal, with no evidence of scar. In the heart with latex-induced infarction that was examined by histofluorescence microscopy, there was absence of catecholamine fluorescence in the area of necrosis and the scintigraphically denervated area, whereas basal regions showed normal nerve fluorescence.

Ligation model. All of the hearts with coronary ligation-induced infarction showed gross evidence of infarction, located primarily in the subendocardium. Histologically, there was subendocardial fibrosis with scattered patchy fibrosis in areas of normal subepicardial myocardium. These patchy areas containing regions with normal histologic findings showed an absence of nerve fluorescence (Fig. 3). As in the hearts injected with latex, the functional maps from hearts after coronary ligation also showed regions of reduced MIBG content relative to thallium (yellow to green), indicating denervation (Fig. 4). The denervated region was usually thin and showed reduced intensity on the functional maps (Fig. 4), consistent with the nontransmural necrosis seen histologically. In general, the region of denervation in these hearts was largely confined to this thin area within the infarct territory, with less extensive involvement of peripheral areas beyond the infarct territory, as was seen in hearts with transmural necrosis (Fig. 2B). Norepinephrine content was significantly reduced in regions showing scintigraphic evidence of denervation compared with the basal areas (74 ± 82 vs. 791 ± 212 ng/g, $p < 0.001$). However, norepinephrine content in regions distal to the infarct area was not significantly different from that of control regions (503 ± 216 vs. 717 ± 265 ng/g).

Sham-operated control dogs. Two of the four sham-operated control dogs showed a mild decrease in MIBG at the apex, a pattern that has been seen in normal dogs (6). However, two other sham-operated dogs showed a mild reduction in MIBG in the anterior wall, consistent with nerve damage. The degree of MIBG reduction in these dogs was displayed as yellow on the functional maps, indicating a level of MIBG 76% of that in the normal region. This reduction was never as severe as that found in the infarcted hearts, which was generally displayed as green, indicating a level of MIBG that was 18% of the normal region. In the total group of sham-operated control dogs, the norepinephrine content was slightly lower in the anterior left ventricle than in the posterobasal area; however, the mean difference did not reach statistical significance (371 ± 177 versus 717 ± 97, $p = 0.06$).

Discussion

Experimental models of myocardial infarction. In a prior study (3), we found histologic evidence of transmural necrosis in six of six dogs with latex injection into the left anterior descending coronary artery, and nontransmural necrosis in nine of nine dogs with ligation of the vessel without latex injection. The histologic results in the current study were similar. Other investigators (12) report that ligation of a coronary artery in dog hearts leads to significant subepicardial sparing of myocardium due to the large degree of collateral circulation in the dog. In contrast, injection of latex into the occluded vessel interrupts collateral flow, and routinely produces dense, transmural necrosis (8). These

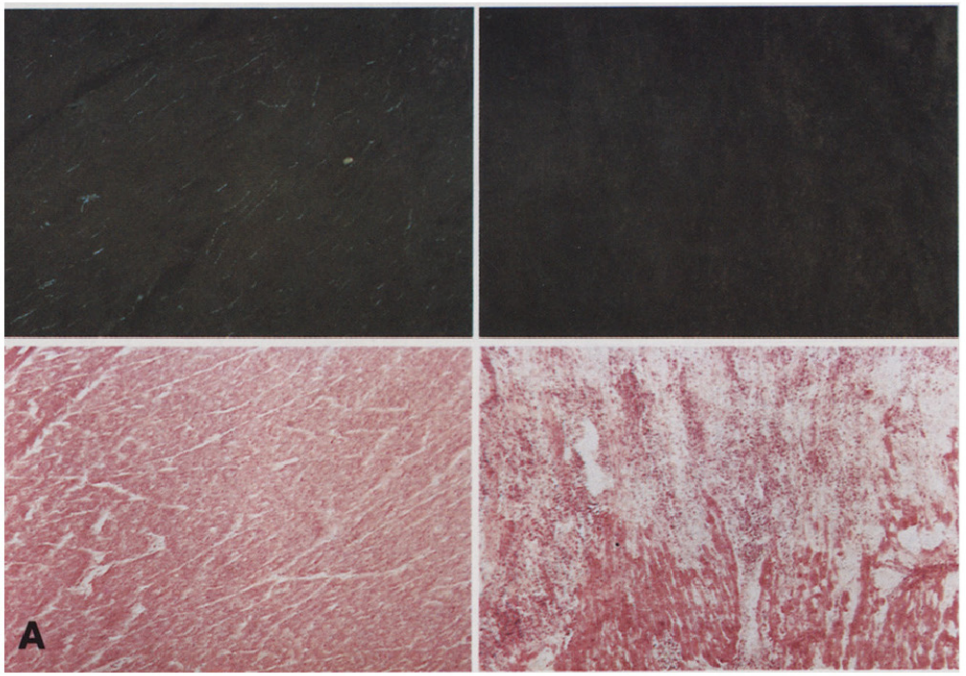

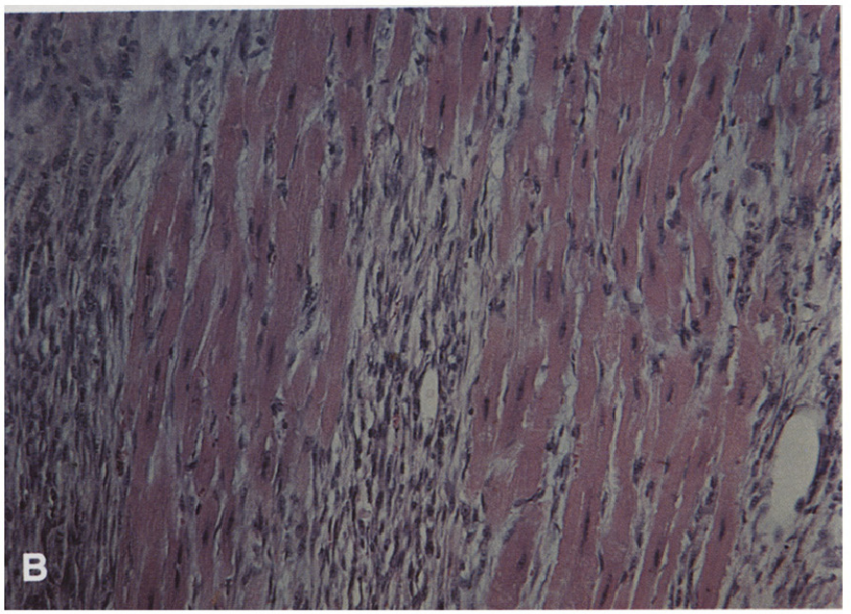

Figure 3. Upper panels. A, Histofluorescence micrographs (**above**) and corresponding histologic sections (**below**) from a normal region localized at the base (**left**) and a region classified histologically as an area of nontransmural infarction with denervation (**right**) in a dog studied 8 days after coronary artery ligation. The nerves are clearly shown as a blue-green fluorescence in the normal basal region (**upper left**), but are absent from the denervated region (**upper right**). The myofibrils show normal histologic findings in the basal region (**lower left**), and patchy fibrosis is seen in the infarcted region (**lower right**) (original magnification ×60). **B,** A higher magnification micrograph of the region classified histologically as nontransmural infarction. Note the normal-appearing myocytes with normal nuclei, and the patchy areas of fibrosis (original magnification ×1,000).

Figure 4. (**left**) Functional maps of myocardial slices from a dog studied 6 days after coronary artery ligation, resulting in a nontransmural infarction. The yellow to green color indicates a greater reduction in MIBG activity in this infarcted zone, indicating denervation. This thin region of reduced intensity (particularly the green area) is within the region of spared subepicardial myocardium seen histologically.

two models of infarction provided reproducible patterns of transmural and nontransmural necrosis, allowing assessment of the effects of infarct type on myocardial innervation.

Scintigraphic assessment of innervation. A previous study (4) demonstrated the affinity of radioiodinated MIBG, an analogue of guanethidine, for the adrenal medullae and adrenergic nerves. MIBG is believed to have uptake and storage mechanisms similar to those of norepinephrine (13), but is not metabolized by monoamine oxidase or catechol-o-methyl transferase. We (6) and others (5) have shown a correlation between MIBG uptake and norepinephrine content in regionally denervated dog hearts. The distribution of MIBG cannot be interpreted as providing a map of myocardial norepinephrine content, however; 80% of the myocardial norepinephrine content is synthesized within the heart itself and is not recaptured (14,15). The distribution of MIBG most closely represents the distribution of sympathetic nerve endings with a preserved uptake process.

Our previous work has validated the accuracy of the computer functional maps in detecting denervated but viable myocardium. In the current study, all of the infarcted hearts showed scintigraphic evidence of denervation to varying degrees. This was evident on the functional maps as a region of yellow to green, indicating decreased MIBG relative to thallium uptake. This scintigraphic appearance correlated with reduced norepinephrine content and absence of sympathetic nerve histofluorescence. The most detailed observations were available from the maps of the excised slices. In these, both transmural and nontransmural infarcts showed evidence of denervation. The transmural lesions showed denervation primarily distal and adjacent to the site of infarction, in a region of myocardium with normal histologic features. This pattern is consistent with the electrophysiologic findings of Barber et al. (2) as well as the scintigraphic and electrophysiologic findings of Minardo et al. (7), in which transmural infarction was shown to produce distal denervation of viable myocardium. These findings are also in agreement with the results of Kozlovshis et al. (16), who found a regional reduction of norepinephrine in nonscarred tissues surrounding the scar in a transmural infarction model in the cat. We did not examine the norepinephrine contents within the region of dense scar; however, there was absence of nerve fluorescence within this region. Also, the absence of perfusion or MIBG uptake in this region on the images makes it highly unlikely that viable nerve terminals were present.

Transmural infarction. Barber et al. (2) demonstrated that transmural infarction produced by vinyl latex injection into a diagonal branch of the left anterior descending coronary artery produced efferent sympathetic and vagal denervation distal to the infarction. The regional application of phenol produced sympathetic but not vagal efferent denervation (17). Because phenol produces only epicardial injury, these differences suggest that sympathetic nerves travel primarily in the epicardium, whereas vagal fibers travel more deeply (17). Barber et al. (2) hypothesized that the necrosis of subepicardial sympathetic nerve trunks in the region of a transmural infarct leads to denervation of distal but viable regions. Our results support this hypothesis. Denervation was routinely present beyond the infarct in the hearts showing transmural lesions.

Nontransmural infarction. The nontransmural infarcts in our study also showed evidence of denervated myocardium. The denervation was primarily localized within the spared subepicardial region of the infarct territory. To our knowledge, this is the first report to describe sympathetic denervation in nontransmural infarction. This finding is in contrast to the results of Kozlovshis et al. (16), who found normal norepinephrine content within areas of nontransmural infarction in a cat model. The reason for this difference in the nontransmural infarcts may relate to the apparently very limited size of the nontransmural infarcts produced by Kozlovshis et al. (16). These infarcts were described as showing a small scar at the subendocardium at the base of the anterior papillary muscle, whereas the lesions that occurred in our dog models showed more diffuse involvement of the subendocardium.

Nontransmural infarcts largely involve the subendocardium and usually preserve the subepicardial layer of myocardium (18), where the sympathetic nerve trunks are located. In this situation, one may anticipate that denervation would not occur. However, all of the nontransmural infarcts showed scintigraphic evidence of denervation. The denervation was present at the subepicardial border of the infarct, a finding that suggests that the distal nerve terminals within the ischemic myocardium were damaged whereas the myocytes were not necrosed. The myocardium *peripheral to* the site of infarction showed little evidence of denervation. This would suggest that the subepicardial nerve trunks supplying the distal areas were spared.

Effect of ischemia in myocardial sympathetic nerves. Local release of norepinephrine from sympathetic nerve endings occurs during myocardial ischemia and has been associated with the development of arrhythmias (19). Few studies have examined the effects of ischemia on the morphology of sympathetic nerves. Although some studies (20) suggest that the sympathetic nerves are resistant to the effects of anoxia, several studies (21,22) show histochemical evidence of nerve damage with diffusion of catecholamines after 30 min to 4 h of ischemia. A slight reduction in catecholamine content also occurs within hours of ischemia, but total depletion of catecholamines takes several days (23). Muntz et al. (24) observed a greater reduction in the percent volume of nerve terminals than in the biochemically measured level of tissue catecholamines after 3 h of ischemia, suggesting that a local release of norepinephrine had occurred. In addition, a patchy distribution of nerve terminals was observed, raising the possibility that sympathetic imbalance may occur in regions of severe ischemia. Our results would suggest that the sympathetic nerves may be more susceptible than cardiac muscle to permanent ischemic damage because of the consistent occurrence of denervation

within nontransmural lesions, with preserved viability of myocytes. In a recent preliminary study (25) in which intracoronary balloon occlusion followed by reperfusion in dogs resulted in subendocardial necrosis, we found evidence of denervation in the surviving subepicardial region as well.

Sham procedures. Two of the sham-operated control dogs showed evidence of mild denervation within the territory of the left anterior descending coronary artery; however, the degree of denervation was never as severe as that noted in the infarcted hearts. MIBG content was reduced 24% compared with that in normal regions in the sham-operated control dogs, whereas in denervated regions in the infarcted hearts it was reduced an average of 82%. This mild reduction in MIBG uptake in the sham-operated group correlated with a mild but not statistically significant reduction in tissue norepinephrine content in the anterior left ventricle. That the denervation in the nontransmural infarcts was primarily located within the infarcted territory and not beyond is further evidence that the denervation in the infarcted hearts was not simply due to manipulation of the vessels. In the two sham-operated control dogs showing evidence of denervation, the coronary artery was deep and required an extensive dissection that probably resulted in trauma to the perivascular nerves. Other investigators (26) have shown evidence of denervation after manipulation of coronary arteries. Extreme caution should be exercised when using open chest models for creating infarction, especially when autonomic effects are to be studied.

Functional implications of denervation: vulnerability to arrhythmias. Our results demonstrate that in experimental myocardial infarction, the relative uptake of MIBG shows a spectrum: no uptake in the center of an infarct with no flow and relatively decreased MIBG uptake in the border zone of an infarct. This border zone may be transmural or nontransmural. The mechanisms leading to the decreased MIBG uptake in each area may be different.

Clinically, most large myocardial infarcts consist of a homogeneous central, transmural area surrounded by a peripheral area of nontransmural infarction. This peripheral area would be expected to be partially denervated either by the necrosis of nerve endings passing through the transmural region or by the necrosis of nerve trunks present within the nontransmural region. Several recent investigations (3,27) show increased susceptibility to induced ventricular fibrillation or ventricular tachycardia in dogs with myocardial infarction and denervation. In a recent preliminary study (28), we compared MIBG/thallium functional maps and measurements of action potential duration in dogs with myocardial infarction. There was significant shortening of action potentials in normally innervated regions during stellate ganglion stimulation but no change in the denervated area. This induced heterogeneity of ventricular action potential duration may be important in the underlying mechanisms related to arrhythmogenesis after myocardial infarction.

Recent studies (29) demonstrate that partial denervation does occur in humans after myocardial infarction. The ability to detect the distribution of innervation scintigraphically and to correlate these imaging findings with electrophysiologic assessment of vulnerability to arrhythmia may provide important new understanding of the interaction of the sympathetic nerves and cardiac pathophysiology. In addition, a noninvasive means may be found to detect patients at risk for sudden death, and possibly provide a basis for more rational approaches to therapy.

The superb technical assistance of Michael C. Chin and the radiopharmaceutical support of John P. Huberty are gratefully acknowledged.

References

1. Manger WM. Adrenergic involvement in cardiac pathophysiology. In: Manger WM, ed. Catecholamines in Normal and Abnormal Cardiac Function. New York: Karger Press, 1982:71–121.
2. Barber MJ, Mueller TM, Henry DP, Felten SY, Zipes DP. Transmural myocardial infarction in the dog produces sympathectomy in noninfarcted myocardium. Circulation 1983;67:787–96.
3. Herre JM, Wetstein L, Lin YL, Mills AS, Dae MW, Thames MD. Effect of transmural versus montransmural myocardial infarction on inducibility of ventricular arrhythmias during sympathetic stimulation in dogs. J Am Coll Cardiol 1988;2:413–21.
4. Wieland DM, Brown LE, Rogers WL, et al. Myocardial imaging with a radioiodinated norepinephrine storage analog. J Nucl Med 1981;22:22–31.
5. Sisson JC, Lynch JJ, Johnson J, et al. Scintigraphic detection of regional disruption of adrenergic neurons in the heart. Am Heart J 1988;116:67–76.
6. Dae MW, O'Connell JW, Botvinick EH, et al. Scintigraphic assessment of regional cardiac adrenergic innervation. Circulation 1989;79:634–44.
7. Minardo J, Tuli M, Mock B, et al. Scintigraphic and electrophysiological evidence of canine myocardial sympathetic denervation and reinnervation produced by myocardial infarction or phenol application. Circulation 1988;78:1008–19.
8. Euler DE, Proud CE, Spear JF, Moore EN. The interruption of collateral blood flow to the ischemic canine myocardium by embolization of a coronary artery with latex: effects on conduction delay and ventricular arrhythmias. Circ Res 1981;49:97–108.
9. Harris AS. Delayed development of ventricular ectopic rhythms following experimental coronary occlusion. Circulation 1950;1:1318–24.
10. Nakajo M, Shimabukuro K, Miyji N, et al. Iodine-131 metaiodobenzylguanidine intra- and extra-vesicular accumulation in the rat heart. J Nucl Med 1986;27:84–9.
11. DeLaTorre JC. An improved approach to histofluorescence using the SPG method for tissue monamines. J Neurosci Meth 1980;3:1–5.
12. Jugdutt BI, Hutchins GM, Bulkley BH, Becker LC. Myocardial infarction in the conscious dog: three-dimensional mapping of infarct, collateral flow, and region at risk. Circulation 1979;60:1141–50.
13. Manger WM, Hoffman BB. Heart imaging in the diagnosis of pheochromocytoma and assessment of catecholamine uptake: teaching editorial. J Nucl Med 1983;24:1194–6.
14. Kopin IJ, Gordon EK. Origin of norepinephrine in the heart. Nature 1963;199:1289.
15. Crout JR. The uptake and release of 3H-norepinephrine by the guinea-pig heart in vivo. Arch Exp Pathol Pharmacol 1964;248:85–98.
16. Kozlovshis PL, Fieber LA, Bassett AC, Cameron JS, Kimura S, Myerburg RJ. Regional reduction in ventricular norepinephrine after healing of experimental myocardial infarction in cats. J Mol Cell Cardiol 1986;18:413–23.
17. Martins JB, Zipes DP. Epicardial phenol interrupts refractory period responses to sympathetic but not vagal stimulation in canine left ventricular epicardium and endocardium. Circ Res 1980;47:33–40.
18. Freifeld AG, Schuster HH, Bulkley BH. Nontransmural versus transmural myocardial infarction: a morphologic study. Am J Med 1983;75:423–32.
19. Corr PB, Gillis RA. Autonomic neural influences on the dysrhythmias resulting from myocardial infarction. Circ Res 1978;43:1–9.

20. Ahonen A, Harkonen M, Juntunen J, Kormano M, Penttils A. Effects of myocardial infarction on adrenergic nerves of the rat heart muscle: a histochemical study. Acta Physiol Scand 1975;93:336–44.
21. Paessens R, Borchard F. Morphology of cardiac nerves in experimental infarction of rat hearts. Virchows Archiv [A] 1980;386:265–78.
22. Holmgren S, Abrahamson T, Almgren O. Adrenergic innervation of coronary arteries and ventricular myocardium in the pig: fluorescence microscopic appearance in the normal state and after ischemia. Basic Res Cardiol 1985;80:18–26.
23. Mathes P, Cowan C, Gudbjarnason S. Storage and metabolism of norepinephrine after experimental myocardial infarction. Am J Physiol 1971;220:27–32.
24. Muntz KH, Hagler HK, Boulas J, Willerson JT, Buja LM. Redistribution of catecholamines in the ischemic zone of the dog heart. Am J Pathol 1984;114:64–78.
25. Dae MW, Chin MC, O'Connell W, et al. Effects of reperfusion on myocardial sympathetic nerves (abstr). Circulation 1989;80(suppl II):II-514.
26. Dolezel S, Gerova M, Hartmannova B, Dostal M, Janexkova H, Vasku J. Cardiac adrenergic innervation after instrumentation of the coronary artery in dog. Am J Physiol 1984;246:H459–69.
27. Inoue H, Zipes DP. Results of sympathetic denervation in the canine heart: supersensitivity that may be arrhythmogenic. Circulation 1987;75: 877–87.
28. Newman D, Munoz L, Chin M, et al. The regional electrophysiologic effects of stellate stimulation on infarcted myocardium (abstr). J Am Coll Cardiol 1989;13:128A.
29. Stanton MS, Tuli MM, Radtke NL, et al. Regional sympathetic denervation after myocardial infarction in humans detected noninvasively using I-123-metaiodobenzylguanidine. J Am Coll Cardiol 1989;14:1519–26.